Study of Structural Morphology and Optical Properties of Nickel Doped Nanostructured Tin Oxide Thin Films

Hamsa Abdul Kareem Hmoud
Ministry of Education/ General Directorate of Education in Baghdad Governorate/ Rusafa Third.
hamsaaljaber@yahoo.com

Abstract:
The article describes a method that was used to prepare thin films of Undoped SnO_2 and SnO_2:Ni thin films via a simple, costless, and suitable technique to prepare thin films with acceptable homogeneity using chemical spray pyrolysis (CSP) method. XRD anaylsis assures that Undoped SnO_2 and SnO_2:Ni films are polycrystalline with recognized peak at (110)., Nickel content were changed from (0 , 2, 4) % cause increasing the crystallite size from 12.76 nm to the Undoped SnO_2 and 14.08 nm for the SnO_2: 4%Ni. while the dislocation density and strain are decreasing from (6.14-5.04) nm, (2.71 – 2.46) nm respectively. Furthermore average diameter decreased from 75.09 nm to 60.78 nm with an increase of Nickel content. R_{rms} value of 6.78 nm for Undoped SnO_2 thin films decreased to 3.16 nm by ni content increase to 4%. The transmittance decreased slightly with increasing of Nickel content, while absorption coefficient is increased with the increasing of Nickel content in SnO_2 films, energy gap decreased from 3.68 eV for SnO_2 film to 3.58 eV for the doping SnO_2: 4% Ni film. refractive index and extinction coefficient are decreased with the increase Nickel content
Keywords: SnO_2: Ni thin films, CSP, XRD, AFM, optical properties.

دراسة الخصائص التركيبية والمورفولوجية والبصرية لأغشية أوكسيد القصدير ذات التراكيب النانوية والمطعم بالنيكل

همسة عبد الكريم حمود
وزارة التربية/ المديرية العامة للتربية في محافظة بغداد/ الرصافة الثالثة

المستخلص
يصف هذا البحث الطريقة التي استخدمت لتحضير أغشية رقيقة من أوكسيد القصدير غير المطعم والمطعم بالنيكل بواسطة تقنية بسيطة وغير مكلفة ومناسبة لتحضير هذه الأغشية بتجانس مقبول وباستخدام تقنية التحلل الكيميائي الحراري. اثبت تحليل حيود الاشعة السينية بان الأغشيةالمحضرة كانت متعددة التبلور مع قمة ملحوظة عند (١١٠). تم تغير محتوى النيكل (٠، ٢، ٤)% وسبب هذا التغير زيادة في الحجم الحبيبي من ١٢,٧٦ نانومتر بالنسبة للأغشية غير المطعمة الى ١٤,٠٨ نانومتر للأغشية المطعمة بـ ٤ % نيكل.كانت كثافة الانخلاعات والمطاوعة تقل من (٦,١٤ – ٥,٠٤) نانومتر و (٢,٧١ – ٢,٤٦) نانومتر على التعاقب. علاوة على ذلك فان معدل القطريقل من ٧٥,٠٩ نانومتر الى ٦٠,٧٨ نانومتر مع زيادة نسبة التطعيم بالنيكل. ان الجذر التربيعي لمعدل الخشونة كان ٦,٧٨ نانومتر واصبح ٣,١٦ نانومترلاغشية المطعمة بـ ٤ % نيكل. قلت النفاذية بشكل قليل مع زيادة التطعيم بالنيكل، بينما معامل الامتصاص يزداد مع زيادة التطعيم بالنيكل. قلت فجوة الطاقة منeV ٣,٦٨ الى eV ٣,٥٨ لأغشية المطعمة ٤ % بالنيكل، ان معامل الانكسار ومعامل الخمود قلت بزيادة نسبة التطعيم بالنيكل.
الكلمات الافتاحية: أغشية SnO_2: Ni، الرش الكيميائي الحراري، XRD ، AFM، الخصائص البصرية.

Introduction

SnO_2 films was studied by many researchers due to their huge applications in industry [1-7]. SnO_2 has a wide bandgap (3.6–3.8 eV) that exhibits an n-type conductivity [8-13].

SnO_2 films was employe as gas sensor owing to high sensitivity and low operating temperatures [14-16]. The system for med by SnO_2 depositedon SiO_2 presents a great interest because of the use of SnO_2/SiO_2 contactsin solar cells [17]. A theoretical conversion efficiency of 2% is predicted for SnO_2/n-Siheterojunctions [18]. Many methods were employed to deposit SnO2:Ni thin films, including CVD [19], sputtering [20], activated reactive evaporation [21], sol gel [22] and CSP [23, 24], The present work is condenced on the preparation of SnO_2 and SnO_2:Ni thin films on the glass bases by spray was employed to study some physical properties of nanostructured SnO_2 films utilizing various Nickel concentrations.

Experimental

Undoped SnO_2 and SnO_2:Ni films were grown by low cost CSP technique. The starting solution was achieved by dissolving 0.1 M of $SnCl_4.5H_2O$ supplied from (BDH Chemicals England) using distilled water to obtain an aqueous solution of the materials used for deposition. The doping material was Nickel trichloride ($NiCl_3$) resolved in redistilled water, drops of HCl were gathered the sol get it homogenous. The optimum condition after many trials have arrived at the following: substrate temperature was 450^{o}C . Distance between spout and base was 30 cm , spraying rate was 5 ml/min, the carrier gas was Nitrogen ,sprayin time was 9 S lasted by 100 S wait to avoid excessive cooling. Gravimetric method was used to obtain thin films of thickness , which was about 330 ± 20 nm. XRD was employed to obtain strucural to measure the structural specifications. AFM was utilized to know the surface topography. Double beam spectrophotometer was employed to obtain transmittance spectra.

Result and discussion

Figure (1) offers XRD styles of the intended films. Peaks were obderved at angles of (2Θ~ ٢٦,٧٣^o, 39.96^o, 54.78^o and 65.97^o) corresponding to the planes (110), (200), (220) and (301) respectively which belong hexagonal structure with the preferred orientation of (110). These peaks are consistent with (ICDD) card number (41-1445).

The average crystallite size (*D*) was estimated employing the equation[25]:

$$\boldsymbol{D = \frac{0.9\,\lambda}{\beta cos\theta}} \qquad \textbf{(1)}$$

Where λ is wavelength of X-rays used (0.1541 nm), β and θ are (FWHM) and the diffraction angle respectively. *D* of the of Undoped SnO_2 films was 12.76 nm and it increases to 14.08 nm with Nickel doping increasing up to 4%

The dislocation density (δ) is calculated using the Eq. (2) [26].

$$\delta = \frac{1}{D^2} \qquad (2)$$

The strain (Ɛ) is calculated using the Eq. (3) [27].

$$\varepsilon = \frac{\beta cos\theta}{4} \qquad (3)$$

The results are offered in Table 1. δ and ε are decreasing from (6.14-5.04) nm, (2.71 – 2.46) nm.

Figure (2) offers each of the FWHM, *D*, δ and ε as a function to the Nickel content.

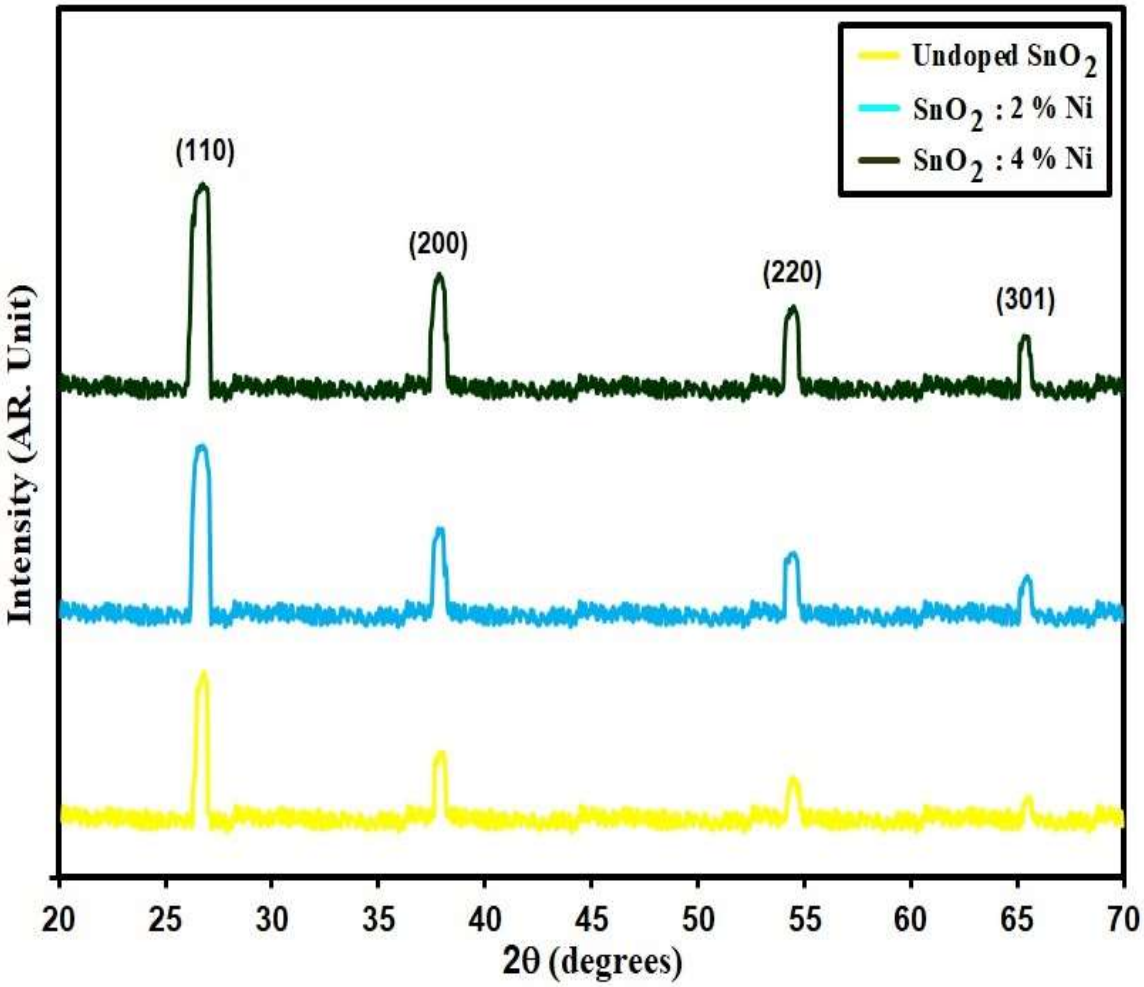

Fig.1. XRD styles of intended films.

Table 1. D, E_g and structural parameters of deposited films.

Samples	2 □ (°)	(hkl) Plane	FWHM (°)	Optical bandgap (eV)	*D* (nm)	Dislocations density (× 10^{15})(lines/m^2)	Strain (× 10^{-3})
Undoped SnO_2	26.73	110	0.64	3.68	12.76	6.14	2.71
SnO_2: 2% Ni	26.71	110	0.62	3.64	13.17	5.76	2.63
SnO_2: 4% Ni	26.68	110	0.58	3.58	14.08	5.04	2.46

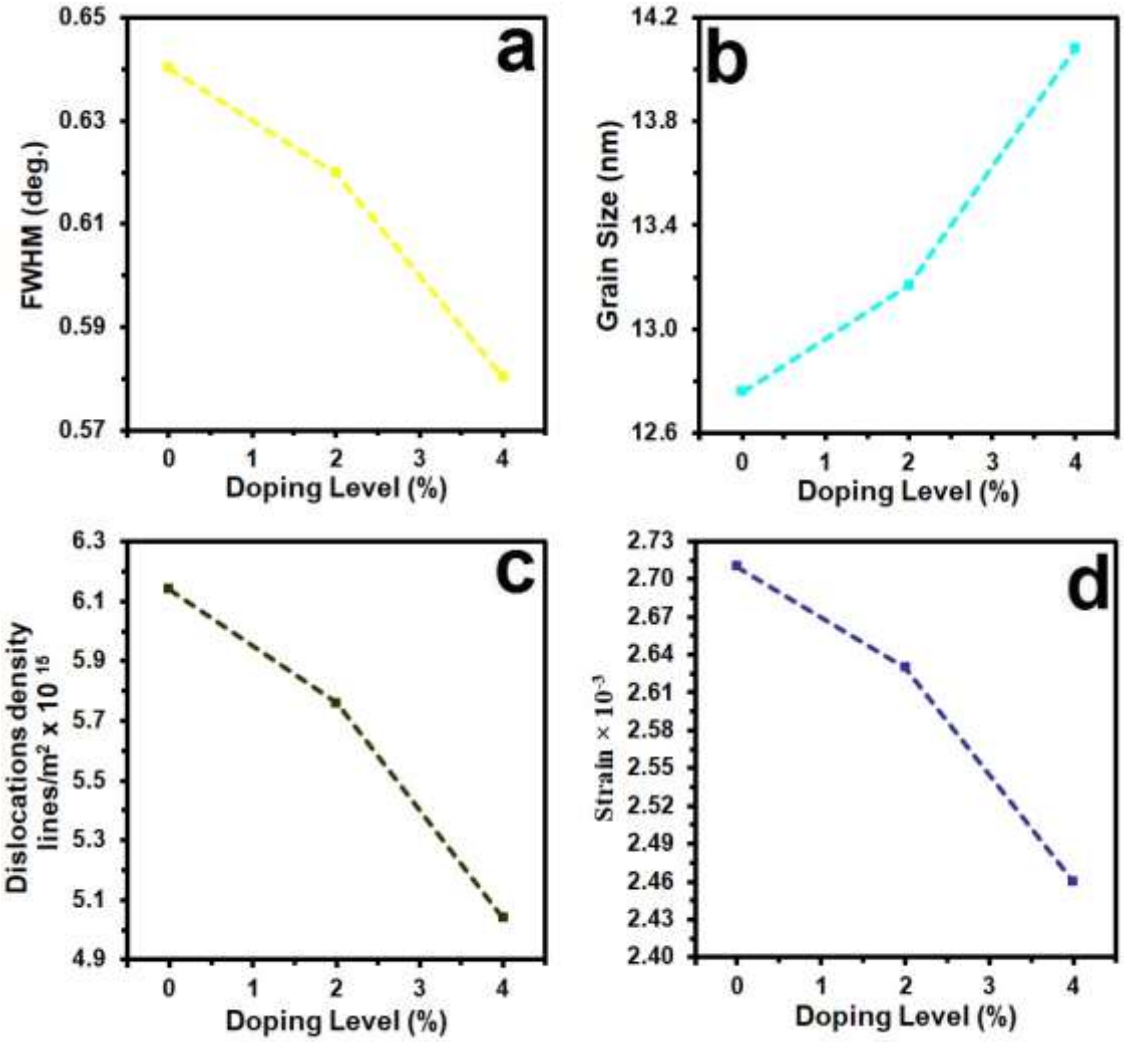

Fig.2. FWHM (a) *D* (b) δ (c) ε (d) of intended films.

Fig. (3) displays AFM image. the Average Particle size P_{av} , root mean square roughness (R_{rms}) and average roughness (R_a) are displayed in Table 2. the Average Particle size was noticed at (75.09), (71.85) and (60.78) nm for the (Undoped SnO_2, SnO_2:2% Ni, SnO_2: 4% Ni) respectively, The Rrms value of 6.78 nm for Undoped SnO_2 thin films decreased to 3.16 nm to SnO_2: 4% Ni, R_a roughness parameters versus dopant content were exhibited in Fig. 3 (a_3, b_3,and c_3) respectively. Table (2) represent the values of AFM parameters P_{AFM}.

Table 2. P_{AFM} of the intended films.

Samples	**P_{av} nm**	**R_a(nm)**	**R_{rms} (nm)**
Undoped SnO_2	75.09	7.89	6.78
SnO_2: 2% Ni	71.85	6.67	6.25
SnO_2: 4% Ni	60.78	6.09	3.16

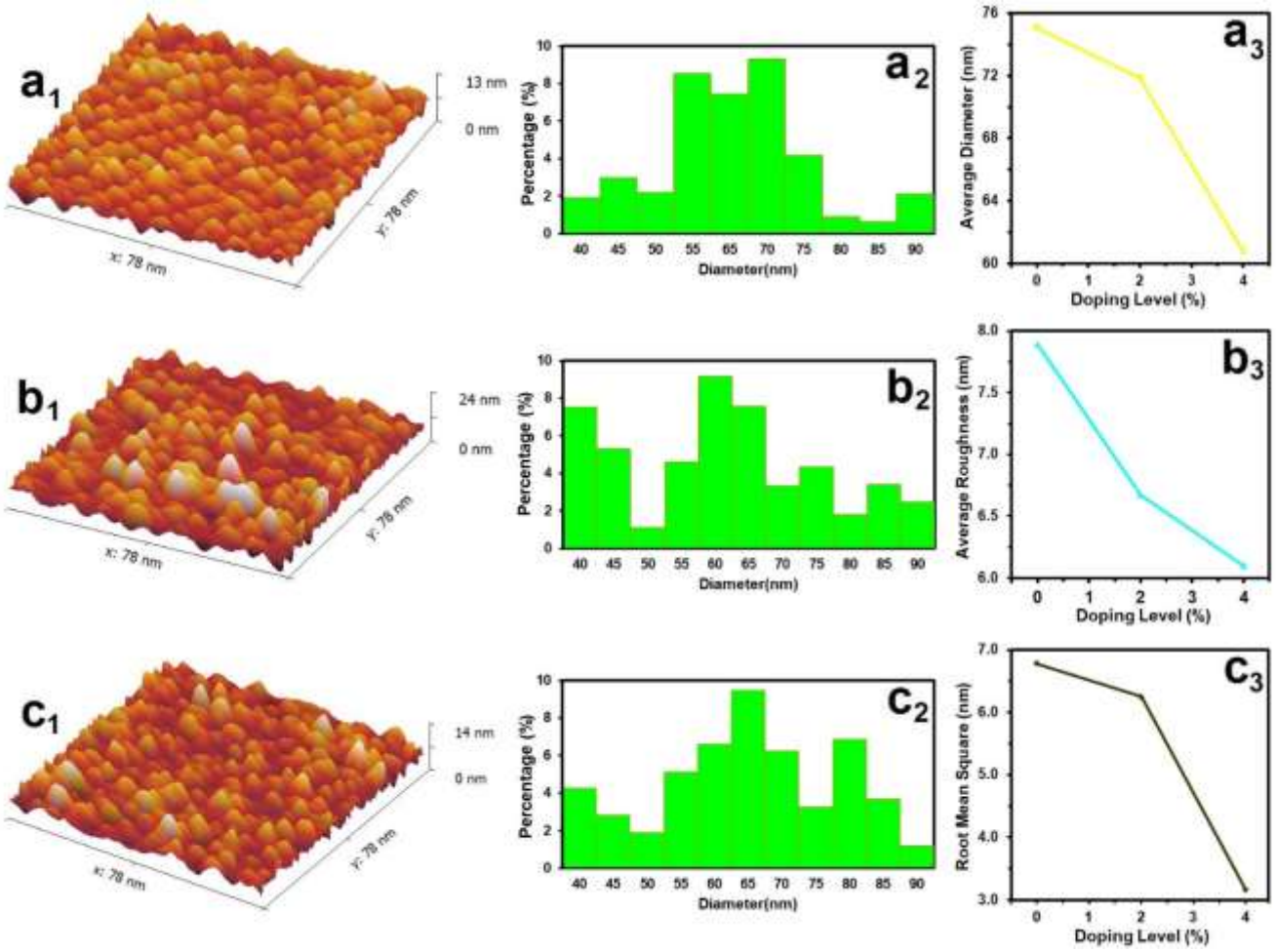

Fig.3. AFM images (a_1, b_1 and c_1), granularly distributed (a_2, b_2 and c_2) and variance of AFM parameters via doping (a_3, b_3 and c_3).

Fig. 4 offers transmittance (t) spectra. From the figure, it can notice that T of Undoped SnO_2 and SnO_2:Ni film decreased with the increase Nickel.

The absorption coefficient (α) is obtained from [28]:

$$\alpha = \ln (1/T)/d \qquad (4)$$

Where, d is film thickness.

α for Undoped SnO_2 and SnO_2:Ni in Fig. 5., Fig. 5. shows the absorption coefficient increase with an increase at 2% or 4% Ni doping.

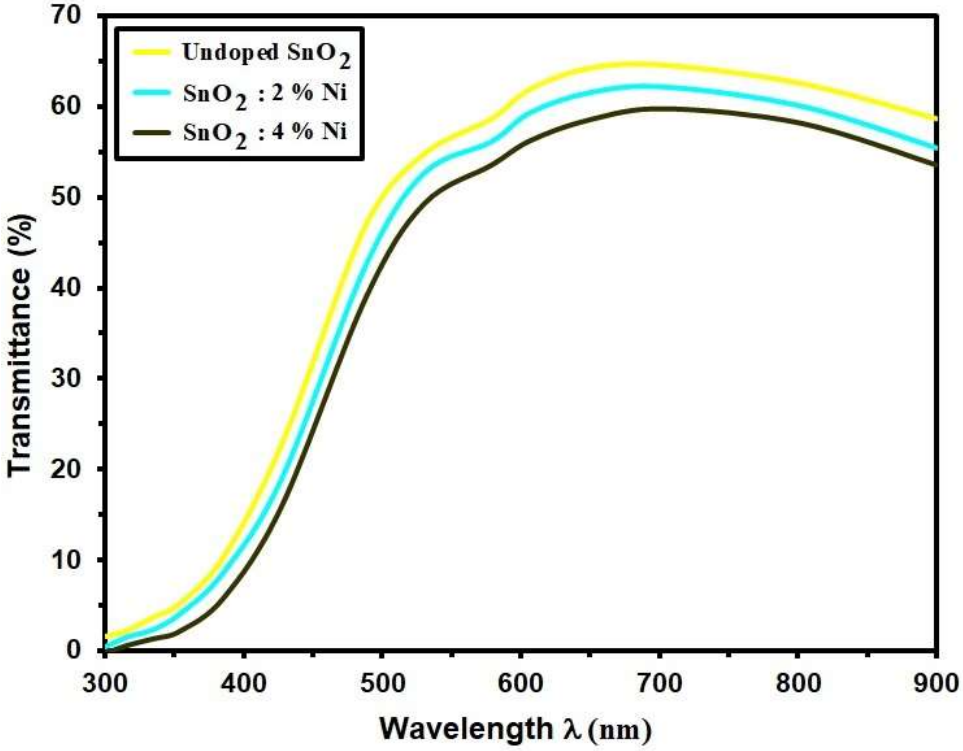

Fig. 4. T of the intended films.

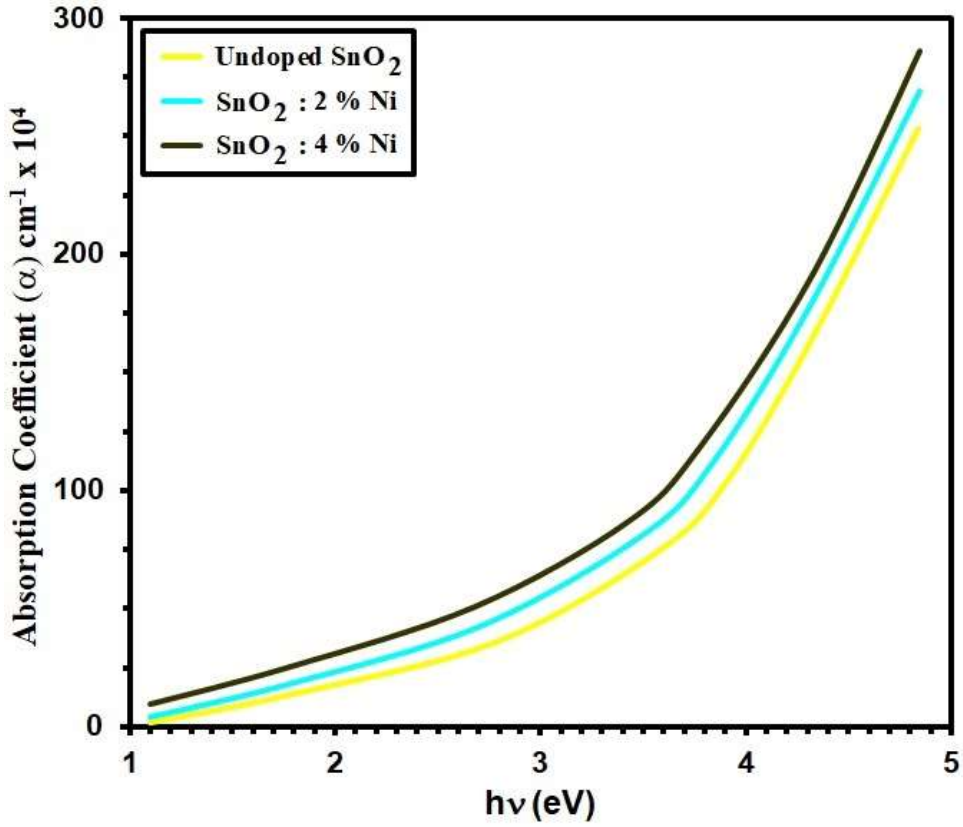

Fig. 5. α Vs hν for intended films.

The optical band gap (E_g) allowing direct transitions was obtained employinr equation 5 [29]:

$$(\alpha h\nu) = A\left(h\nu - E_g\right)^{\frac{1}{2}} \qquad (5)$$

Where A is the constant, E_g is illustrated in Fig. 6. E_g values of the Undoped SnO_2, SnO_2:2% Ni and SnO_2: 4% Ni thin films are found to be about 3.68, 3.64 and 3.58 eV respectively. Table (1) offers the values of E_g.

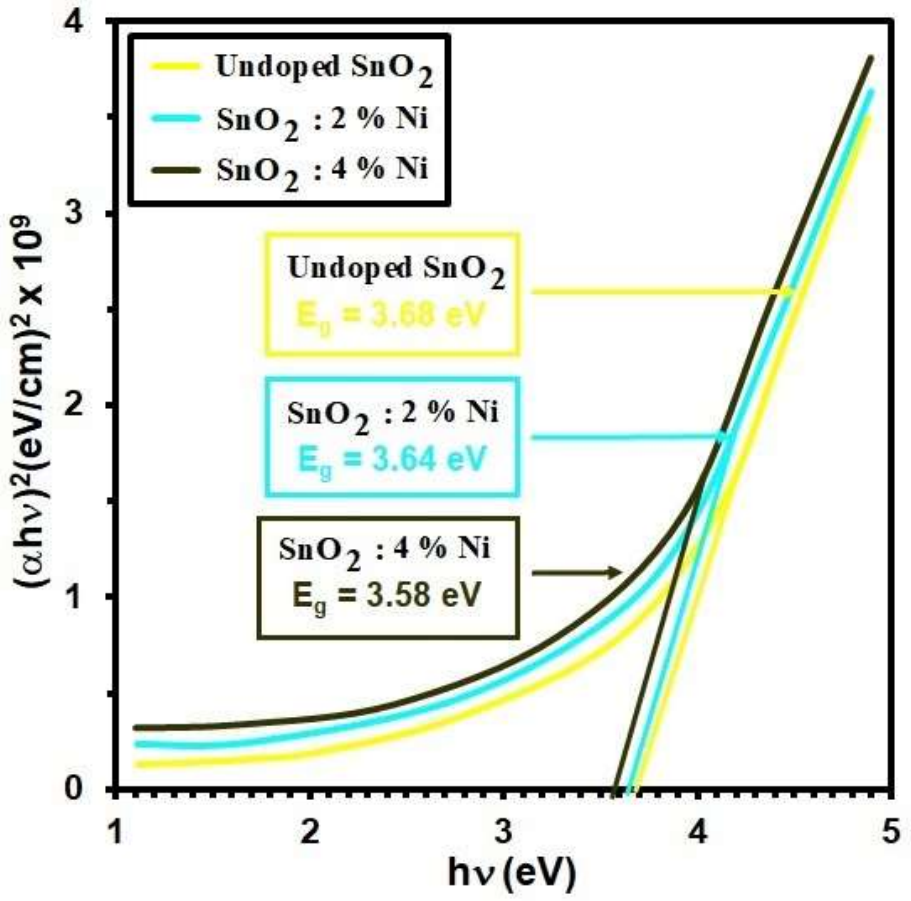

Fig. 6. $(\alpha h\nu)^2$ Vs hν of intended films.

The extinction coefficient (k) is shown in Fig.7, which can be calculated by the following equation [31, 32]:

$$k = \frac{\alpha\lambda}{4\pi} \text{ ----- (7)}$$

Where λ is the wavelength. The extinction coefficient decreased with the increasing the content of Nickel.

The refractive index (n) is calculated by using the equation [33, 34]:

$$n = \left(\frac{1+R}{1-R}\right) + \sqrt{\frac{4R}{(1-R)^2} - k^2} \text{ ----- (8)}$$

Where R is the reflectivity. Fig. 8 represent the relationship between the refractive index with the wavelength. Refractive index decreases with the increasing the content of Nickel.

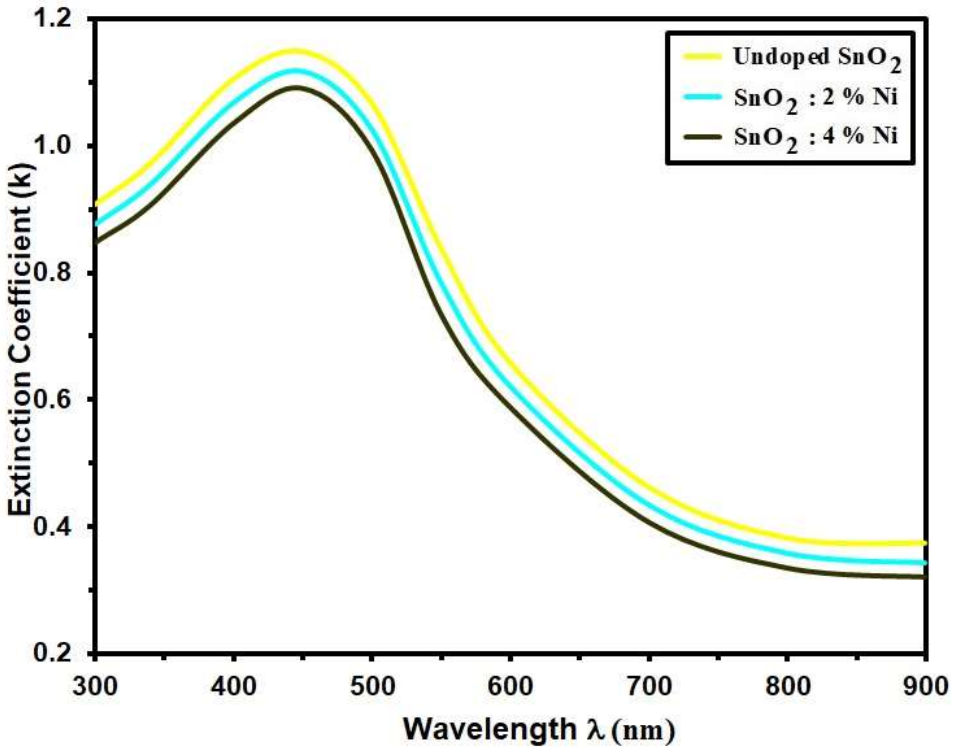

Fig. 7. extinction coefficient of intended films.

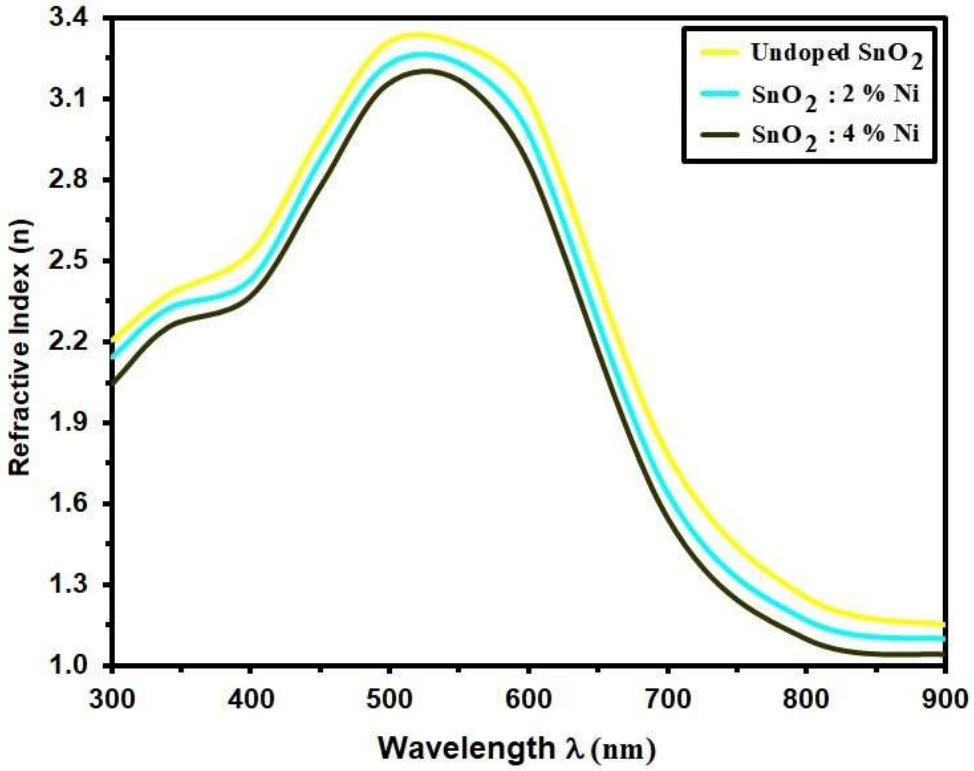

Fig.٨ . refractive index of intended films.

Conclusion

A simple and convenient spray pyrolysis technique method was deposited Undoped SnO_2 and SnO_2:Ni thin films on commercial glass at various concentrations of Nickel. XRD anaylsis assures the polycrystallinity with prefereed peak at (110). *D* increases from 12.76 nm to 14.08 nm as Nicke lcontent increase. Whilist strain parameter decreased from 2.71 to 2.46, Surface morphology study shows that higher concentration of Lithium doped CuS thin films were of high quality, AFM studies revealed that R_{rms} values decrease from 6.78 nm to 3.16 nm from the film Undoped SnO_2 and SnO_2:4% Ni. AFM image showed that grain size from 75.09 nm to 60.78 nm with Undoped SnO_2 and SnO_2:4% Ni. The transmittance decreased slightly with an increase of Nickel content in SnO_2 films. The optical properties approve that E_g increased from 3.68 -3.58 eV at 4% Ni doping. extinction coefficient and refractive index decreased with the increase Nickel.

References

[1] Fan S, Zhang J, Teng X, Wang X, Li H, Li Q, Xu J, Cao D, Li Shandong and Hu H, Self-Supported Amorphous SnO_2/TiO_2 Nanocomposite Films with Improved Electrochemical Performance for Lithium-Ion Batteries, Journal of The Electrochemical Society, 2019,166 (13): A3072-A3078 .

[2] Zhang S, Yin C, Yang L, Zhang Z and Han Z, Investigation of the H_2 sensing properties of multilayer mesoporous pure and Pd-doped SnO_2 thin film, Sensors and Actuators B: Chemical, 2019, 283: 399-406

[3] Zhang, B, et al., T he FTIR studies of SnO_2: In (ATO) films deposited by spray pyrolysis, Materials Letters, 2011, 65.8: 1204-1206.

[4] Liu K, Zhang R, Wu M, Jiang H and Zhao T, Ultra-stable lithium plating/stripping in garnet-based lithium-metal batteries enabled by a SnO_2 nanolayer, Journal of Power Sources, 2019, 433: 226691.

[5] Melo S, Rodríguez E O. Galán V, Hernández-Gutiérrez C A, Pulgarín-Agudelo F A and Mendoza-León H, Deposition of SnO_2 buffer layer onto commercial conducting glass to be used in thin films solar cells technology, Superficies y Vacío, 2018, 31 (4): 63-68.

[6] Ameur S B, hadjltaief H B, Barhoumi A, Duponchel B, Leroy G, Amlouk M and Guermazi H, Physical investigations and photocatalytic activities on ZnO and SnO_2 thin films deposited on flexible polymer substrate, Vacuum, 2018,155: 546-552.

[7] Satoh K, Yamada Y, Kanaoka Y, Murakami S, Kakehi Y and Sakurai Y, Investigation on the gate insulator thickness dependence of ZnO–SnO_2 thin film transistors, Japanese Journal of Applied Physics, 201958 (3): 038004.

[8] Singh R et al., Effects of In, Zn doping on structural, electrical and optical properties of SnO_2 thin films, Materials Science in Semiconductor Processing, 2015,31: 310-314.

[9] Wang C-M, et al, Investigation of pulsed ultraviolet laser annealing of In/SnO_2 thin films on the structural, optical and electrical properties, Surface and Coatings Technology, 2013, 231: 374-379.

[10] Ao D and Ichimura M. Deposition and characterization of In and Cu doped nanocrystalline SnO_2 thin films fabricated by the photochemical method, Journal of Non-Crystalline Solids, 2012: 358 (17): 2470-2473.

[11] Floriano E A, et al., Decay of photo-induced conductivity in In-doped SnO_2 thin films, using monochromatic light of about bandgap energy, Applied Surface Science, 2013, 267: 164-168.

[12] Lekshmy S S, Georgi P D and Joy K, Microstructure and physical properties of sol gel derived SnO_2: In thin films for optoelectronic applications, Applied Surface Science, 2013, 274: 95-100.

[13] Geraldo V, et al. Drude's model calculation rule on electrical transport in In-doped SnO_2 thin films, deposited via sol–gel, Journal of Physics and Chemistry of Solids, 2006, 67 (7): 1410-1415.
[14] Messias F R, et al, Electron scattering and effects of sources of light on photoconductivity of SnO_2 coatings prepared by sol–gel, Journal of non-crystalline solids, 1999, 247 (1-3): 171-175.
[15] Khadayeir A A, Hassan E S, Chiad S S, Habubi N F, Abass K H, Rahid M H, Mubarak T H, Dawod M O and Al-Baidhany I A, Structural and Optical Properties of Boron Doped Cadmium Oxide, Journal of Physics: Conference Series, 2019,1234: 012014.
[16] Hassan E S, Mubarak T H, Abass K H, Chiad S S, Habubi N F, Rahid M H, Khadayeir A A, Dawod M O and Al-Baidhany Ismaeel A, Structural, Morphological and Optical Characterization of Tin Doped Zinc Oxide Thin Film by (SPT), Journal of Physics: Conference Series, 2019,1234: 012013.
[17] Srivastava A, et al., Study of structural and microstructural properties of SnO_2 powder for LPG and CNG gas sensors, Materials chemistry and physics, 2006, 97 (1): 85-90.
[18] Kojima M, et al., Transparent furnace made of heat mirror, Thin Solid Films, 2001, 392 (2): 349-354.
[19] Kane J, chweizer H P S and Kern W, Chemical Vapor Deposition of Antimony- Doped Tin Oxide Films Formed from Dibutyl Tin Diacetate, Journal of the Electrochemical Society, 1976,123 (2): 270-277.
[20] Vossen J L and Poliniak E S, The properties of very thin RF sputtered transparent conducting films of SnO_2: In and In_2O_3: Sn, Thin Solid Films, 1972, 13 (2): 281-284.
[21] evaporation, Thin Solid Films, 1981, 83 (2): 267-271.
[22] Scherrer P, Estimation of the size and internal structure of colloidal particles by means of röntgen. Nachr. Ges. Wiss. Göttingen 2 (1918): 96-100.
[23] Afi H H, Momtz R S, Badawy W A and Nasser S A, J. Mat. So. Mat. Electonics, 1991, 2: 40.
[24] Blandenet G, Court M and Lagarde Y, Thin layers deposited by the pyrosol process, Thin Solid Films, 1981,77 (1-3): 81-90.
[25] Cullity B D, Addison-Wesley Publications Company Inc. Reading, Massachusetts (1956).
[26] Orel B, et al, Structural and FTIR spectroscopic studies of gel-xerogel-oxide transitions of SnO_2 and SnO_2: In powders and dip-coated films prepared via inorganic sol-gel route, Journal of non-crystalline solids, 1994, 167 (3): 272-288.
[27] Tauc J, Grigorovici R and Vancu A, Optical properties and electronic structure of amorphous germanium, physica status solidi (b), 1966,15 (2): 627-637.
[28] Kim, H W and Shim S H, Synthesis and characteristics of SnO_2 needle-shaped nanostructures, Journal of alloys and compounds, 2006, 426(1-2): 286-289.
[30] Lokhande C D, Ubale A U and Patil P S, Thickness dependent properties of chemically deposited Bi_2S_3 thin films, Thin Solid Films, 1997, 302 (1-2): 1-4.
[31] Gorley P M, et al., SnO_2 films: formation, electrical and optical properties, Materials Science and Engineering, B1, 2005,18 (1-3): 160-163.
[32] Bayansal F., et al, Growth of homogenous CuO nano-structured thin films by a simple solution method, Journal of Alloys and Compounds, 2011, 509 (5): 2094-2098.
[33] Shanthi E, Dutta V, Banerjee A and Chopra K L, Electrical and optical properties of undoped and antimony-doped tin oxide films, J. Appl. Phys., 1980,51: 6243–6251.
[34] Jow-Lay Huang, Din-Wen Kuo, and Bor-Yuan Shew, "The effects of heat treatment on the gas sensitivity of reactively sputtered SnO2 films", Surface and Coatings Technology 79 (1996) 263-267.